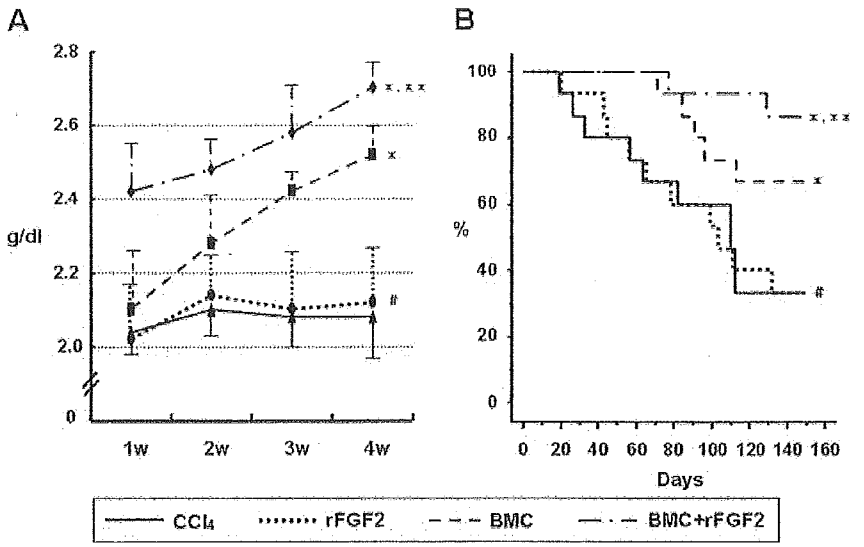

Fig. 5 Effect of rFGF2 treatment with BMT (*CCl_4* treatment with neither BMCs nor rFGFs, *rFGF2* rFGF2-only treatment without BMT, *BMC* BMC-only transplantation without rFGFs, *BMC+ rFGF2* treatment with both BMCs and rFGF2). **A** Time-course of serum albumin level. Serum albumin level is most significantly elevated by rFGF2 treatment in combination with BMT among four groups. *Significant difference compared with the value at the same period in the CCl_4 group ($P<0.05$). **Significant difference compared with the value at the same period in the BMC group ($P<0.05$). #No significant difference compared with the value at the same period in the CCl_4 group ($P>0.05$). **B** Cumulative survival analysis evaluated by the Kaplan-Meier method. Administration of rFGF2 with BMT improves the survival rate, which is significantly the highest among the four groups. *Significant difference compared with CCl_4 group ($P<0.05$). **Significant difference compared with BMC group ($P<0.05$). #No significant difference compared with CCl_4 group ($P>0.05$)

highest among the four groups ($P<0.05$). On the other hand, there was no significant difference between the CCl_4 group and rFGF2 group. These data suggest that administration of rFGF2 in combination with BMT is significantly the most effective for mice with damaged liver.

TNF-α signaling is activated by BMT with rFGF2 treatment

To improve our understanding of the molecular mechanism of the effect of FGF2 on the enhancement of the repop-

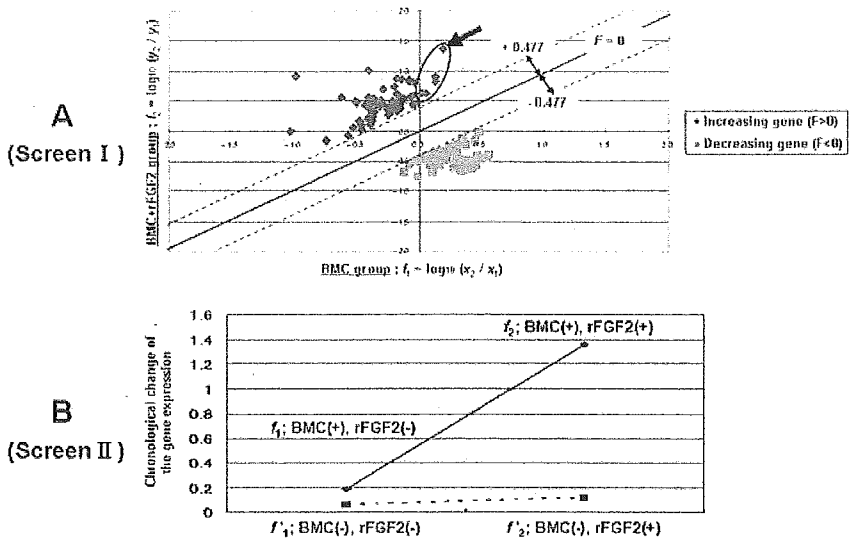

Fig. 6 Identification of the specific gene involved in repopulation and differentiation by using DNA-microarray analysis and two screens. **A** Plot of genes in the f_1–f_2 space (*Screen I*). The five specific genes out of 1108 genes are selected in screen I (*encircled plots* the five selected genes, *large arrow* TNFIP3). **B** Chronological change of the gene expression of TNFIP3 (*Screen II*). TNFIP3 is most specifically activated by treatment with both BMCs and rFGF2 compared with others in Screen II. The *f* value represents the chronological change of the expression level of a gene in each group (*f1';BMC(−),rFGF2(−)* CCl_4 group treated with neither BMCs nor rFGFs, *f2';BMC(−),rFGF2 (+)* rFGF2-only treatment without BMT, *f1;BMC(+),rFGF2(−)* BMC-only transplantation without rFGFs, *f2;BMC(+),rFGF2(+)* treatment with both BMCs and rFGF2)

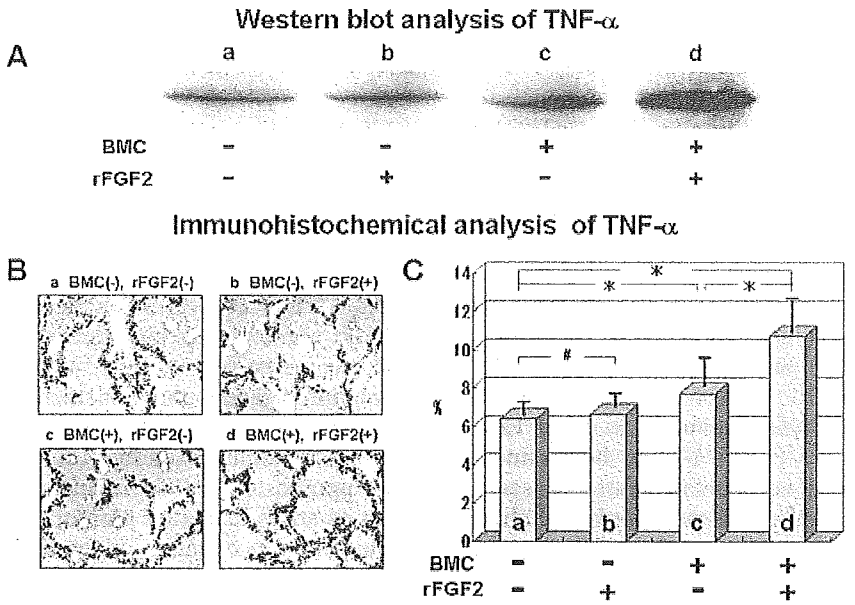

Fig. 7 Expression of TNF-α in CCl_4, rFGF2, BMC, and BMC+ rFGF2 groups (*a* CCl_4 group: treatment with neither BMCs nor rFGFs, *b* rFGF2 group: rFGF2-only treatment without BMT, *c* BMC group: BMC-only transplantation without rFGFs, *d* BMC+rFGF2 group: treatment with both BMCs and rFGF2). **A** Western blot analysis of TNF-α. The level of TNF-α expression in BMC+rFGF2 group is the highest amongst the four groups in immunoblot analysis. **B** Immunohistochemical analysis of TNF-α. Expression of TNF-α slightly increases with BMT-alone and is significantly elevated by rFGF2 treatment in combination with BMT compared with other treatments. ×40 **C** Percentage of stained area of TNF-α. The BMC+rFGF2 group shows the highest percentage of stained area of TNF-α amongst the four groups. *Significant difference between two groups ($P<0.05$). #No significant difference between two groups ($P>0.05$)

ulation and differentiation of BMCs in the GFP/CCl_4 model, we used microarray analysis to profile the chronological change in gene expression before and after rFGF2 treatment. We carried out two screens to identify the specific gene that was activated by rFGF2 treatment in combination with BMT in mice with CCl_4-induced liver damage. Figure 6A shows the plot of genes in the 2-dimensional space spanned by f_1 and f_2 in screen I. We could select five genes that fulfilled the conditions $f_1>0$, $f_2>0$ and $F>0.477$ ($=\log_{10}3$), out of 1,108 genes. These specific genes are TNF-α induced protein 3 (TNFIP3), hypoxia-inducible factor 1α, neural plakophilin-related arm-repeat protein, semaphorin B, and zinc-finger protein 46. Screen II was performed to separate the gene that was most specifically up-regulated by rFGF2 treatment with BMT out of five genes selected from screen I. In this analysis, TNFIP3 was most significantly activated when BMT and treatment with rFGF2 were combined compared with others (Fig. 6B). We next analyzed the expression of TNF-α protein in the liver from four groups at 1 week after transplantation: the CCl_4 group, rFGF2 group, BMC group, and BMC+rFGF2 group. Immunoblot analysis (Fig. 7A) revealed that BMT itself slightly elevated TNF-α expression, and the level of TNF-α expression in the BMC+rFGF2 group was the highest amongst the four groups. Immunohistochemical analysis confirmed the results of the immunoblot (Fig. 7B,C). Treatment of rFGF2 without BMT, by contrast, did not activate TNF-α signaling in our system. Together, these results suggest that FGF2 significantly activates TNF-α signaling during the process of the differentiation of BMCs into hepatocytes.

Discussion

A number of reports have demonstrated the potential of BMCs to differentiate into a variety of cell types, including hepatocytes (Theise et al. 2000; Orlic et al. 2001; Ferrari et al. 1998; Lagasse et al. 2000; Krause et al. 2001; Kotton et al. 2001; Petersen et al. 1999; Okamoto et al. 2002). We have previously developed an in vivo model, the GFP/CCl_4 mouse model, and have reported that transplanted BMCs differentiate into albumin-producing functional mature hepatocytes via Liv2-positive immature hepatoblast intermediates (Terai et al. 2003). Furthermore, BMT elevates the serum albumin level, reduces liver fibrosis, and improves the survival rate in our model (Sakaida et al. 2004). The mechanism behind the BMC plasticity that we have observed in the model is the subject of much debate. For example, the mechanism could reportedly involve cell fusion, nuclear reprogramming, or trans-differentiation (Terada et al. 2002; Ying et al. 2002; Ianus et al. 2003; Hochedlinger et al. 2004; Harris et al. 2004; Jang et al. 2004), and several lines of evidence have led us to believe that both cell fusion and trans-differentiation might be important to BMC plasticity. We have previously performed microarray analysis (using specific equations with SOM) to analyze the molecular cues that controlled the differentiation of BMCs into hepatocytes in GFP/CCl_4

model and found a dramatic change of gene expression during BMC differentiation (Omori et al. 2004). In the early stage after BMT, genes known to regulate morphology, such as homeobox, helix-loop-helix transcription factors, and FGFs are up-regulated. In later stages, however, the genes that show relatively increased levels can be categorized as those associated with hepatocyte differentiation, such as hepatocyte nuclear factor-4 and glucose-6-phosphatase isomerase (Omori et al. 2004).

Several growth factors have previously been reported to play important roles in the repair processes in myocardium, vessel, nerve, skin, and bone (Detillieux et al. 2003; Kowalczyk and Pasyk 2002; Werner and Grose 2003; Goodman et al. 2003). Indeed, clinical trials of various growth factors (e.g., FGF, VEGF, HGF) for the treatment of peripheral vascular disorders, ischemic heart diseases, and cutaneous chronic wounds have been performed (Laham et al. 2000; Lederman et al. 2002; Fu et al. 2002). In this study, we have analyzed the expression of several growth factors and their receptors during the process of the repopulation and differentiation of BMCs into hepatocytes. We have found that the expression of FGFs and FGFRs significantly increases with time after BMT compared with other factors, and that the expression levels of FGFs and FGFRs are significantly higher in the BMT(+) group than in the BMT(−) control group ($P<0.05$; Figs. 1, 2, Table 1). These results suggest that the FGF-FGFR system is important in our GFP/CCl_4 model. Furthermore, transplanted GFP-positive BMCs express both FGFs and FGFRs (Fig. 3). Our data indicate that transplanted BMCs differentiate into hepatocytes under the control of autocrine regulation by FGF signaling in the model system. These findings agree well with previous studies showing that FGF is crucial for the initial process of liver development (Kinoshita and Miyajima 2002; Jung et al. 1999; Deutsch et al. 2001). Indeed, a previous microarray-SOM analysis in our laboratory has demonstrated that FGF is an important factor at an early stage in the GFP/CCl_4 model (Omori et al. 2004). Taken together, these reports support our current finding that FGF-FGFR signaling plays important roles, especially during the early differentiation of BMCs into hepatocytes.

We have also investigated the way that the administration of rFGF affects the repopulation and differentiation of BMCs into hepatocytes in the GFP/CCl_4 model. Treatment with rFGF, especially rFGF2, significantly elevates the repopulation rate of GFP-positive cells in the liver and increases the expression of both Liv2 and albumin ($P<0.05$; Fig. 4, Table 2). Furthermore, the serum albumin level is significantly elevated ($P<0.05$; Fig. 5A), and the survival rate is significantly improved ($P<0.05$; Fig. 5B) by treatment with rFGF2 in combination with BMT. In our present microarray analysis and screen I, we have been able to identify specific five genes that are significantly activated by BMT together with rFGF2 treatment compared with BMT-alone (Fig. 6A). In addition, as shown in Fig. 6B, screen II has revealed that TNFIP3 is most specifically up-regulated by rFGF2 treatment in combination with BMT amongst the five genes identified by screen I. Interestingly, the induction of TNFIP3 (also called as A20) has been reported to be caused by TNF-α stimulation, and A20 is involved in feedback suppression of nuclear factor-κB (NF-κB) activation induced by TNF-α (Idel et al. 2003). We have not been able to obtain information regarding TNF-α expression itself, because our microarray system does not include it. We have lastly confirmed the expression of TNF-α protein during the differentiation of BMCs in GFP/CCl_4 model mice. BMT-alone slightly elevates TNF-α expression, and moreover, the level of TNF-α expression is significantly the highest when BMT and treatment with rFGF2 are combined, as shown by immunoblot and immunohistochemical analysis (Fig. 7). TNF-α is a pluripotent mediator that affects several cellular processes, including adhesion, migration, angiogenesis, and apoptosis. TNF-α-regulated inflammation signals, such as stress-activated protein kinase/extracellular signal regulated-kinase kinase 1/mitogen-activated protein-kinase kinase 4-mediated c-jun NH_2-terminal kinase signaling, are important for the generation of hepatoblasts (Watanabe et al. 2002). Yamada and Fausto (1998) have shown that the TNF receptor 1 signaling pathway involving NF-κB, interleukin-6, and the signal transducer and activator of transcription 3, is an important component of the hepatocyte mitogenic response induced by CCl_4 injury in mouse liver. From these reports and our present studies, we speculate that the transplantation of BMCs and concurrent treatment with rFGF2 has a synergistic effect that facilitates or potentiates the differentiation of transplanted BMCs into hepatocytes through the activation of TNF-α signaling.

In conclusion, we have found that FGF2 is the most important growth factor in the GFP/CCl_4 model of liver damage and regenerative treatment. Our present studies suggest that FGF2 facilitates the differentiation of transplanted BMCs into albumin-producing hepatocytes via Liv2-positive hepatoblast intermediates through the activation of TNF-α signaling. Additionally, administration of FGF2 in combination with BMT improves the liver function and prognosis of mice with CCl_4-induced liver damage and might thus have the potential to become an effective and efficient therapy for patients with severe liver disease.

Acknowledgements We thank Dr. Masaru Okabe (Genome Research Center, Osaka University) for the gift of GFP transgenic mice and Mr. Jun Oba for valuable technical support.

References

Alison MR, Poulsom R, Jeffery R, Dhillon AP, Quaglia A, Jacob J, Novelli M, Prentice G, Williamson J, Wright NA (2000) Hepatocytes from non-hepatic adult stem cells. Nature 406:257

Detillieux KA, Sheikh F, Kardami E, Cattini PA (2003) Biological activities of fibroblast growth factor-2 in the adult myocardium. Cardiovasc Res 57:8–19

Deutsch G, Jung J, Zheng M, Lora J, Zaret KS (2001) A bipotential precursor population for pancreas and liver within the embryonic endoderm. Development 128:871–881

Ferrari G, Cusella-De Angelis G, Coletta M, Paolucci E, Stornaiuolo A, Cossu G, Mavilio F (1998) Muscle regeneration by bone marrow-derived myogenic progenitors. Science 279:1528–1530

Fu X, Shen Z, Guo Z, Zhang M, Sheng Z (2002) Healing of chronic cutaneous wounds by topical treatment with basic fibroblast growth factor. Chin Med J (Engl) 115:331–335

Goodman SB, Song Y, Yoo JY, Fox N, Trindade MC, Kajiyama G, Ma T, Regula D, Brown J, Smith RL (2003) Local infusion of FGF-2 enhances bone ingrowth in rabbit chambers in the presence of polyethylene particles. J Biomed Mater Res 65A:454–461

Harris RG, Herzog EL, Bruscia EM, Grove JE, Van Arnam JS, Krause DS (2004) Lack of a fusion requirement for development of bone marrow-derived epithelia. Science 305:90–93

Hochedlinger K, Blelloch R, Brennan C, Yamada Y, Kim M, Chin L, Jaenisch R (2004) Reprogramming of a melanoma genome by nuclear transplantation. Genes Dev 18:1875–1885

Ianus A, Holz GG, Theise ND, Hussain MA (2003) In vivo derivation of glucose-competent pancreatic endocrine cells from bone marrow without evidence of cell fusion. J Clin Invest 111:843–850

Idel S, Dansky HM, Breslow JL (2003) A20, a regulator of NFkappaB, maps to an atherosclerosis locus and differs between parental sensitive C57BL/6J and resistant FVB/N strains. Proc Natl Acad Sci U S A 100:14235–14240

Ishigaki S, Niwa J, Ando Y, Yoshihara T, Sawada K, Doyu M, Yamamoto M, Kato K, Yotsumoto Y, Sobue G (2002) Differentially expressed genes in sporadic amyotrophic lateral sclerosis spinal cords–screening by molecular indexing and subsequent cDNA microarray analysis. FEBS Lett 531:354–358

Jang YY, Collector MI, Baylin SB, Diehl AM, Sharkis SJ (2004) Hematopoietic stem cells convert into liver cells within days without fusion. Nat Cell Biol 6:532–539

Jung J, Zheng M, Goldfarb M, Zaret KS (1999) Initiation of mammalian liver development from endoderm by fibroblast growth factors. Science 284:1998–2003

Kinoshita T, Miyajima A (2002) Cytokine regulation of liver development. Biochim Biophys Acta 1592:303–312

Kollet O, Shivtiel S, Chen YQ, Suriawinata J, Thung SN, Dabeva MD, Kahn J, Spiegel A, Dar A, Samira S, Goichberg P, Kalinkovich A, Arenzana-Seisdedos F, Nagler A, Hardan I, Revel M, Shafritz DA, Lapidot T (2003) HGF, SDF-1, and MMP-9 are involved in stress-induced human CD34+ stem cell recruitment to the liver. J Clin Invest 112:160–169

Kotton DN, Ma BY, Cardoso WV, Sanderson EA, Summer RS, Williams MC, Fine A (2001) Bone marrow-derived cells as progenitors of lung alveolar epithelium. Development 128: 5181–5188

Kowalczyk J, Pasyk S (2002) Vascular endothelial growth factor and its application in therapy of cardiovascular diseases. Pol Merkuriusz Lek 13:74–78

Krause DS, Theise ND, Collector MI, Henegariu O, Hwang S, Gardner R, Neutzel S, Sharkis SJ (2001) Multi-organ, multilineage engraftment by a single bone marrow-derived stem cell. Cell 105:369–377

Lagasse E, Connors H, Al-Dhalimy M, Reitsma M, Dohse M, Osborne L, Wang X, Finegold M, Weissman IL, Grompe M (2000) Purified hematopoietic stem cells can differentiate into hepatocytes in vivo. Nat Med 6:1229–1234

Laham RJ, Chronos NA, Pike M, Leimbach ME, Udelson JE, Pearlman JD, Pettigrew RI, Whitehouse MJ, Yoshizawa C, Simons M (2000) Intracoronary basic fibroblast growth factor (FGF-2) in patients with severe ischemic heart disease: results of a phase I open-label dose escalation study. J Am Coll Cardiol 36:2132–2139

Lederman RJ, Mendelsohn FO, Anderson RD, Saucedo JF, Tenaglia AN, Hermiller JB, Hillegass WB, Rocha-Singh K, Moon TE, Whitehouse MJ, Annex BH (2002) Therapeutic angiogenesis with recombinant fibroblast growth factor-2 for intermittent claudication (the TRAFFIC study): a randomised trial. Lancet 359:2053–2058

Okamoto R, Yajima T, Yamazaki M, Kanai T, Mukai M, Okamoto S, Ikeda Y, Hibi T, Inazawa J, Watanabe M (2002) Damaged epithelia regenerated by bone marrow-derived cells in the human gastrointestinal tract. Nat Med 8:1011–1017

Omori K, Terai S, Ishikawa T, Aoyama K, Sakaida I, Nishina H, Shinoda K, Uchimura S, Hamamoto Y, Okita K (2004) Molecular signature associated with plasticity of bone marrow cell under persistent liver damage by self-organizing-map-based gene expression. FEBS Lett 578:10–20

Orlic D, Kajstura J, Chimenti S, Jakoniuk I, Anderson SM, Li B, Pickel J, McKay R, Nadal-Ginard B, Bodine DM, Leri A, Anversa P (2001) Bone marrow cells regenerate infarcted myocardium. Nature 410:701–705

Petersen BE, Bowen WC, Patrene KD, Mars WM, Sullivan AK, Murase N, Boggs SS, Greenberger JS, Goff JP (1999) Bone marrow as a potential source of hepatic oval cells. Science 284:1168–1170

Sakaida I, Terai S, Yamamoto N, Aoyama K, Ishikawa T, Nishina H, Okita K (2004) Transplantation of bone marrow cells reduces CCl4-induced liver fibrosis in mice. Hepatology 40:1304–1311

Shinoda K, Mori S, Ohtsuki T, Osawa Y (1992) An aromatase-associated cytoplasmic inclusion, the "stigmoid body," in the rat brain. I. Distribution in the forebrain. J Comp Neurol 322:360–376

Stamm C, Westphal B, Kleine HD, Petzsch M, Kittner C, Klinge H, Schumichen C, Nienaber CA, Freund M, Steinhoff G (2003) Autologous bone-marrow stem-cell transplantation for myocardial regeneration. Lancet 361:45–46

Terada N, Hamazaki T, Oka M, Hoki M, Mastalerz DM, Nakano Y, Meyer EM, Morel L, Petersen BE, Scott EW (2002) Bone marrow cells adopt the phenotype of other cells by spontaneous cell fusion. Nature 416:542–545

Terai S, Sakaida I, Yamamoto N, Omori K, Watanabe T, Ohata S, Katada T, Miyamoto K, Shinoda K, Nishina H, Okita K (2003) An in vivo model for monitoring trans-differentiation of bone marrow cells into functional hepatocytes. J Biochem (Tokyo) 134:551–558

Theise ND, Nimmakayalu M, Gardner R, Illei PB, Morgan G, Teperman L, Henegariu O, Krause DS (2000) Liver from bone marrow in humans. Hepatology 32:11–16

Wang X, Ge S, McNamara G, Hao QL, Crooks GM, Nolta JA (2003) Albumin-expressing hepatocyte-like cells develop in the livers of immune-deficient mice that received transplants of highly purified human hematopoietic stem cells. Blood 101:4201–4208

Watanabe T, Nakagawa K, Ohata S, Kitagawa D, Nishitai G, Seo J, Tanemura S, Shimizu N, Kishimoto H, Wada T, Aoki J, Arai H, Iwatsubo T, Mochita M, Satake M, Ito Y, Matsuyama T, Mak T, Penninger J, Nishina H, Katada T (2002) SEK1/MKK4-mediated SAPK/JNK signaling participates in embryonic hepatoblast proliferation via a pathway different from NF-kappaB-induced anti-apoptosis. Dev Biol 250:332–347

Werner S, Grose R (2003) Regulation of wound healing by growth factors and cytokines. Physiol Rev 83:835–870

Wexler SA, Donaldson C, Denning-Kendall P, Rice C, Bradley B, Hows JM (2003) Adult bone marrow is a rich source of human mesenchymal "stem" cells but umbilical cord and mobilized adult blood are not. Br J Haematol 121:368–374

Yamada Y, Fausto N (1998) Deficient liver regeneration after carbon tetrachloride injury in mice lacking type 1 but not type 2 tumor necrosis factor receptor. Am J Pathol 152:1577–1589

Yamamoto N, Terai S, Ohata S, Watanabe T, Omori K, Shinoda K, Miyamoto K, Katada T, Sakaida I, Nishina H, Okita K (2004) A subpopulation of bone marrow cells depleted by a novel antibody, anti-Liv8, is useful for cell therapy to repair damaged liver. Biochem Biophys Res Commun 313:1110–1118

Ying QL, Nichols J, Evans EP, Smith AG (2002) Changing potency by spontaneous fusion. Nature 416:545–548

J Hepatobiliary Pancreat Surg (2005) 12:203–207
DOI 10.1007/s00534-005-0977-0

Journal of HBP Surgery

Lesson from the GFP/CCl4 model — Translational Research Project: the development of cell therapy using autologous bone marrow cells in patients with liver cirrhosis

Shuji Terai[1], Isao Sakaida[1], Hiroshi Nishina[2], and Kiwamu Okita[1]

[1]Department of Molecular Science and Applied Medicine (Gastroenterology and Hepatology), Yamaguchi University School of Medicine, 1-1-1 Minami Kogushi, Ube, Yamaguchi 755-8505, Japan
[2]Department of Developmental and Regenerative Biology, Medical Research Institute, Tokyo Medical and Dental University, Tokyo, Japan

Abstract
The plasticity of bone marrow has been confirmed by the analysis of autopsy findings in female recipients of bone marrow cells transplanted from male donors. To establish new clinical cell therapies using autologous bone marrow cells for patients with liver failure, we developed a new in vivo model, the "green fluorescent protein (GFP)/carbon tetrachloride (CCl_4) model". Using the GFP/CCl_4 model, we found that transplanted Liv8-negative cells efficiently repopulated into cirrhotic liver tissue and trans-differentiated into albumin-producing hepatocytes under conditions of persistent liver damage induced by CCl_4. Moreover, one marrow cell transplantation into liver cirrhosis mice improved their liver function, ameliorated liver fibrosis, and improved their survival rate. Results from the GFP/CCl_4 model showed that cell therapy using autologous bone marrow cells has the potential to become an effective treatment for patients with liver failure. Here we describe the findings from the GFP/CCl_4 model and the scope of the translational research project.

Key words Bone marrow cells · Bone marrow cell transplantation · Liver cirrhosis · GFP (green fluorescent protein)/carbon tetrachloride (CCl_4) model · Liver fibrosis · Stem cell · Translational research · Trans-differentiation · Niche · Liver fibrosis

Introduction

Liver failure in patients with liver cirrhosis with endstage chronic liver disease is very difficult to cure. At present, liver transplantation is one effective therapy for curing these patients; however, this treatment faces serious problems, such as lack of donors, operative damage, rejection, and high expense. On the other hand, cell transplantation therapy is a minimally invasive procedure with fewer potential complications. Regenerative medicine using stem cells is an attractive therapy for the cure of patients with severe liver disease. The capacity of bone marrow cells (BMCs) to differentiate into hepatocytes and intestinal cells was confirmed through the detection of the Y chromosome in the analysis of autopsy findings in human female recipients of BMCs from male donors.[1–4] BMCs are an attractive cell source for regenerative medicine, because it is easier to obtain BMCs than it is to obtain other tissue-specific stem cells.[5,6] BMC transplantation is also an established treatment for hematological diseases. Clinical studies have evaluated the use of BMCs in regenerating the myocardium and vessels in patients with heart failure and those with limb ischemia.[7–10] Based on these findings, we began to focus on BMCs as a new cell source for liver regenerative therapy. The mechanism of BMC plasticity was previously examined with respect to cell fusion[11,12] and trans-differentiation.[13,14] We think that the most important aspect of developing a new clinical therapy using BMCs is evaluating its effectiveness for liver disease. We think both cell fusion and trans-differentiation could be important for furthering the understanding of the mechanisms of BMC plasticity. Indeed, the development of an effective cell therapy using BMCs requires better understanding of events in the recipient mouse liver after BMC transplantation. We developed a new in vivo model, named the "green fluorescent protein (GFP)/carbon tetrachloride (CCl_4) model",[15] in which to monitor the differentiation of BMCs into functional hepatocytes. Here, we describe the newest findings from the GFP/CCl_4 model. These lessons will be important for proceeding with the translational project of cell therapy using autologous BMCs to treat patients with liver cirrhosis.

The GFP/CCl_4 model

First, we sought to understand how to use BMCs to repair liver damage, using our GFP/CCl_4 model.[15] In the

Offprint requests to: S. Terai
Received: February 14, 2005 / Accepted: February 28, 2005

model, 0.5 ml/kg of CCl_4 is administered twice weekly to C57BL/6 female mice to induce liver cirrhosis, and then GFP-positive BMCs obtained from GFP-Tg mice (C57BL6/Tg14 (act-EGFP) OsbY01 mice)[16] are transplanted through the caudal vein (donor and recipient mice are of the same strain). In this model, we transplanted 1×10^5 GFP-positive BMCs that had not been cultured. By analyzing GFP-positive BMCs in the recipient mice, we evaluated the repopulation and differentiation of BMCs under conditions of continuous liver injury. Immunostaining, using anti-GFP antibodies,[17] showed that GFP-positive BMCs migrated into the marginal area of hepatic lobules, starting 1 day after BMC transplantation; with time, the distribution of GFP-positive BMCs expanded,[15,18] with they formed a hepatic cord towards the central vein. The use of Liv2, a hepatoblast-specific antibody that we developed,[19] also showed that BMCs first trans-differentiated into Liv2-positive hepatoblasts and then differentiated into albumin-positive hepatocytes. Furthermore, the level of serum albumin significantly increased with time in the recipient mice. These findings suggest that the GFP/CCl_4 model can be used to understand the process of BMC differentiation into hepatocytes. On the other hand, GFP-positive cells were not detected in the liver tissues of control mice (those with no liver damage) following BMC transplantation. The persistent liver damage induced by CCl_4 injection is important for producing a specific differentiation "niche" in order to activate the plasticity of BMCs and their subsequent differentiation into hepatocytes. Oval cells were thought to be one type of hepatic stem cells derived from the Canal of Hering following severe liver damage.[20,21] Based on the finding of Petersen et al.,[22] that, under some conditions, oval cells are derived from bone marrow cells, we also analyzed the activation of oval cells, using a specific oval-cell marker, A6 antibody. A6-Positive cells were detected in the periportal region 1 week after BMC transplantation in the GFP/CCl_4 model, but these A6-positive oval cells did not increase in the 4 weeks after BMC transplantation in this model. We could not detect A6-positive cells that also expressed GFP in the liver after BMC transplantation. These results suggest that, while some signals that activate oval cells are induced by BMC transplantation into CCl_4-induced cirrhotic liver, the oval cells may not be derived from transplanted BMCs. In summary, BMCs transplanted into the GFP/CCl_4 model trans-differentiated into hepatoblast phenotypes and differentiated into albumin-producing hepatocytes in the "differentiation niche" created by the persistent cirrhosis induced by CCl_4 injection.

Characteristics of candidate BMCs for cell therapy of liver disease

Although various theories explain the existence of pluripotent stem cells in BMCs, the exact composition of the stem cells in BMCs is not clear at present. The following cell types are known to exist in bone marrow: hematopoietic stem cells (HSCs),[13,23] side population cells (SPCs),[24] and mesenchymal stem cells (MSCs).[25] Although past studies used existing antibodies and techniques, there have not been any studies based on the findings of natural liver development studies. The liver functions as a metabolic organ, with the exception of a short period during the fetal stage from embryonic day (E) 12 to 16 (E12–E16), when the liver functions as a hematopoietic organ.[26] We decided to analyze the usefulness of various cell populations of BMCs, based on the analysis of fetal liver development. We prepared a new monoclonal antibody, anti-Liv8 antibody, which recognizes hematopoietic cells using a specific cell-surface marker, in order to identify and separate subpopulations of BMCs capable of differentiating into hepatocytes under CCl_4-induced continuous liver damage in the GFP/CCl_4 model.[15] Next, we investigated Liv8-positive cells in the BMCs of adult GFP Tg mice. Liv8-positive cells were present in bone marrow in adult GFP-Tg mice; around 32% of BMCs were Liv8-positive. With regard to the relationship between Liv8 and CD45, we found, by flow cytometry, that CD45-positive cells expressed Liv8. These results show that anti-Liv8 is a useful antibody for separating hematopoietic and non-hematopoietic cells. Liv8-positive cells are thought to be hematopoietic cells and Liv8-negative cells are thought to be non-hematopoietic cells. The separated cells were then transplanted into a CCl_4-induced liver damage recipient model. At 4 weeks after BMC transplantation, more efficient repopulation and trans-differentiation of BMCs into hepatocytes was seen with Liv8-negative cells. These findings suggest that the subpopulation of Liv8-negative cells includes cells useful for performing cell therapy in damaged livers.[18]

Improvements in liver function and survival rate, and amelioration of liver fibrosis by BMC transplantation

Using the GFP/CCl_4 model, we also evaluated the recovery of liver function and the effect on liver fibrosis and survival rate. Transplanted BMCs trans-differentiated into albumin-producing hepatocytes, leading to an increase in the serum albumin level. Interestingly, we found an amelioration of liver fibrosis after BMC transplantation.[27] Although the exact mechanism of the fibrolysis remains unclear, transplanted BMCs migrated along fibers that had strong expression of matrix metalloproteinase (MMP)-9, resulting in the resolu-

tion of fibrosis. The degradation of the extracellular matrix presumably led to improved liver function, resulting in the better survival of mice following BMC transplantation. We also analyzed differences in liver fibrosis following the transplantation of Liv8-positive or Liv8-negative BMCs. Our results showed that Liv8-negative BMC transplantation ameliorated liver fibrosis to a greater extent than Liv8-positive BMC transplantation. These results show that subpopulations of Liv-8-negative cells will be useful for treating liver cirrhosis. We think that BMC transplantation into liver cirrhosis mice has two effects: BMC trans-differentiation into albumin-producing hepatocytes and the recovery of liver fibrosis.[18,27] These effects of BMC transplantation accelerate the improvement of liver function and the survival rate.

Molecular mechanisms that regulate the trans-differentiation of BMCs into hepatocytes in the GFP/CCl4 model (microarray-self-organizing map [SOM] analysis)

Recently, cell fusion has been reported to be an important mechanism for the trans-differentiation of BMCs and tissue stem cells.[11,12] The differentiation of BMCs into hepatocytes in the fumarylacetoacetate hydrolase (FAH) model was thought to show the importance of cell fusion in the differentiation of HSCs into hepatocytes.[28,29] However, other groups have reported little evidence of in vivo cell fusion during the trans-differentiation of BMCs into other cell lineages.[14,30] We analyzed the cell fusion rate, using cultured Neo-resistant Embryonic stem (ES) cells and GFP-positive BMCs under the same culture conditions as those used by Terada et al.[11] (cell fusion rate of $1/10^5$–10^6), and found similar cell fusion rates in our in vitro assay (data not shown). Mouse hepatocytes have ploidy values of 2N, 4N, 8N, or 16N. The cell fusion of diploid (2N) BMCs with hepatocytes produces cells with ploidy values of 4N, 6N, 10N, or 18N.[28,29] We were afraid that the variety in ploidy values would make it very difficult to analyze cell fusion. We analyzed the DNA ploidy patterns of primary hepatocytes isolated from mice with livers with persistent CCl_4 damage, with and without BMC transplantation, at 4 weeks. We were able to isolate around 1.2×10^8 hepatocytes from recipient mice at 4 weeks by a two-step collagenase method, and we analyzed DNA ploidy patterns by fluorescence activated cell sorting (FACS), We found 2N, 4N, 8N, and 16N DNA bands. Comparisons of these DNA ploidy patterns showed that the 2N and 4N bands were similar, but the peaks, representing 8N and 16N bands, were slightly different (data not shown). These results show that cell fusion may have occurred in the GFP/CCl_4 model. Next, we analyzed the differentiation of transplanted BMCs into hepatocytes. Although we could not neglect the possibility that cell fusion had occurred in our model, the BMCs trans-differentiated into Liv2-positive hepatoblasts and functional hepatocytes. We think that the trans-differentiation of BMCs actually occurred in the GFP/CCl_4 model. We analyzed the mechanism of this plasticity using DNA chips, which are recently developed tools of genetic analysis. While it is possible to obtain vast amounts of genetic data with DNA chips,[31] interpretation of the factors involved in gene expression requires the application of a statistical technique such as the SOM to visualize the vast amounts of complicated and multidimensional data.[32] In this analysis, we made a specific equation to identify genes that regulate the trans-differentation of BMCs into hepatocytes. In the GFP/CCl_4 model, genes related to morphology were dramatically activated at an early stage, while genes associated with hepatocyte differentiation were upregulated at a later state. In the early stage after BMC transplantation, we found that genes such as *FGF* and c-*kit*, as well as *HOX* and *HLH* transcription factors, might be important. In later stages, genes associated with metabolic function, such as hepatocyte nuclear factor 4 (*HNF4*) and glucose-6-phosphatase (*G6Pase*) isomerase were induced, suggesting that, at 4 weeks after BMC transplantation, the transplanted BMCs had begun to assume some of the metabolic functions of hepatocytes.[33] Although many details remain unconfirmed, we think that the microarray-SOM analysis for the GFP/CCl_4 model confirms the idea that the BMCs trans-differentiated into immature cells and then differentiated into mature hepatocytes. This information will be useful for understanding the mechanism of BMC plasticity in the GFP/CCl_4 model.

Summary of the lessons learned from the GFP/CCl_4 model, and brief report of a clinical study of autologous BMC transplantation into patients with liver cirrhosis

We summarized the findings from the GFP/CCl_4 model. As shown in Fig. 1, transplanted GFP-positive BMCs (especially the Liv8-negative cell population, without culturing) migrated into the periportal regions of the cirrhotic liver. With time, the transplanted GFP-positive BMCs trans-differentiated into Liv2-positve hepatoblasts and then differentiated into albumin-producing hepatocytes. The transplanted BMCs formed a hepatic cord. The differentiation "niche" created by the persistent liver damage caused by continuous CCl_4 injection is a key factor. Microarry-SOM analysis showed that, at an early stage after BMC transplanta-

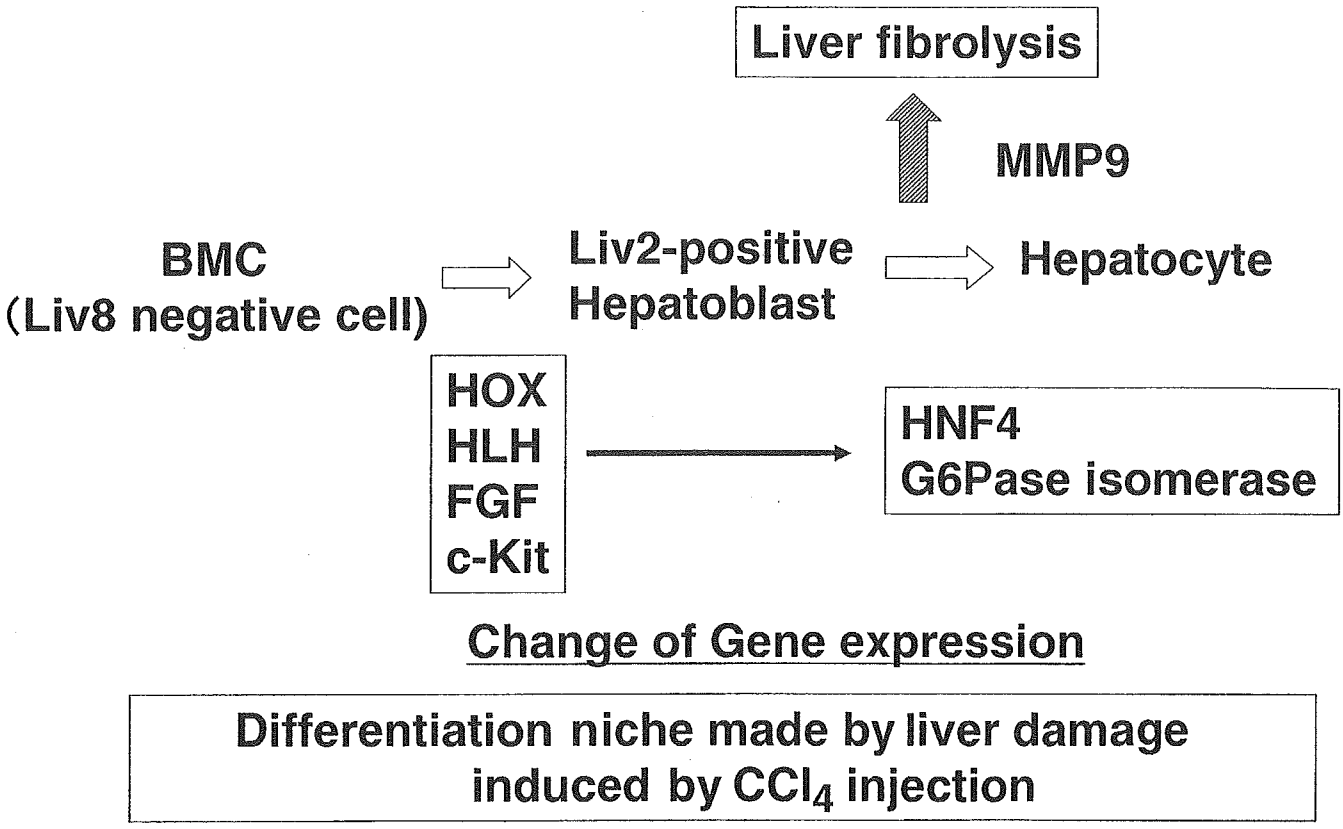

Fig. 1. Summary of the green fluorescent protein/carbon tetrachloride (*GFP/CCl_4*) model. *BMC*, bone marrow cell; *MMP-9*, matrix metalloproteinase-9; *G6Pase*, glucose-6-phosphatase; *HNF4*, hepatocyte nuclear factor 4

tion, the genes related to morphology were activated, and later, genes associated with liver metabolism were activated. Finally, BMC transplantation improved liver function, ameliorated liver fibrosis, and improved the survival rate. These findings strongly support the development of a new cell therapy, using BMCs, to cure liver cirrhosis, especially because autologous BMC transplantation has few ethical problems and BMC transplantation itself is already an established treatment for hematological diseases. Based on the results obtained in basic research using the GFP/CCl_4 model, we prepared a clinical study. We started a phase I clinical study called "Autologous BMC transplantation for liver cirrhosis patients", on November 14, 2003. The study is a first and important step toward the development of a new cell therapy to cure liver failure. We will report the outcome of the phase I clinical study at a later time, and we will combine the basic and clinical studies as part of our translational research, in order to develop a new therapy to cure liver cirrhosis.

Acknowledgments. This study was supported by Grants-in-Aid for Scientific Research from the Japan Society for the Promotion of Science (Nos. 13470121, 13770262, 15790348, 16390211, and 16590597) and by a Grant for Translational Research from the Ministry of Health, Labor and Welfare (H-trans-5) of Japan.

References

1. Alison MR, Poulsom R, Jeffery R, Dhillon AP, Quaglia A, Jacob J, Novelli M (2000) Hepatocytes from non-hepatic adult stem cells. Nature 406:257
2. Theise ND, Nimmakayalu M, Gardnre R, Illei PB, Morgan G, Teperman L, Henegariu O (2000) Liver from bone marrow in humans. Hepatology 32:11–16
3. Korbling M, Katz RL, Khanna A, Ruifrok AC, Rondon G, Albitar M, Champlin RE (2002) Hepatocytes and epithelial cells of donor origin in recipients of peripheral-blood stem cells. N Engl J Med 346:738–746
4. Okamoto R, Yajima T, Yamazaki M, Kanai T, Mukai M, Okamoto S, Ikeda Y (2002) Damaged epithelia regenerated by bone marrow-derived cells in the human gastrointestinal tract. Nat Med 8:1011–1017
5. Terai S, Yamamoto N, Omori K, Sakaida I, Okita K (2002) A new cell therapy using bone marrow cells to repair damaged liver. J Gastroenterol 37(Suppl XIV):162–163
6. Orlic D, Kajstura J, Chimenti S, Jakoniuk I, Anderson SM, Li B, Pickel J (2001) Bone marrow cells regenerate infarcted myocardium. Nature 410:701–705

7. Stamm C, Westphal B, Kleine HD, Petzsch M, Kittner C, Klinge H, Schumichen C (2003) Autologous bone-marrow stem-cell transplantation for myocardial regeneration. Lancet 361:45–46
8. Wexler SA, Donaldson C, Denning-Kendall P, Rice C, Bradley B, Hows JM (2003) Adult bone marrow is a rich source of human mesenchymal "stem" cells but umbilical cord and mobilized adult blood are not. Br J Haematol 121:368–374
9. Hamano K, Li TS, Kobayashi T, Hirata K, Yano M, Kohno M, Matsuzaki M (2002) Therapeutic angiogenesis induced by local autologous bone marrow cell implantation. Ann thorac Surg 73:1210–1215
10. Tateishi-Yuyama E, Matsubara H, Murohara T, Ikeda U, Shintani S, Masaki H, Amano K (2002) Therapeutic angiogenesis for patients with limb ischaemia by autologous transplantation of bone-marrow cells: a pilot study and a randomised controlled trial. Lancent 360:427–435
11. Terada N, Hamazaki T, Oka M, Hoki M, Mastalerz DM, Nakano Y, Meyer EM (2002) Bone marrow cells adopt the phenotype of other cells by spontaneous cell fusion. Nature 416:542–545
12. Ying QL, Nichols J, Evans EP, Smith AG (2002) Changing potency by spontaneous fusion. Nature 416:545–548
13. Krause DS, Theise ND, Collector MI, Henegariu O, Hwang S, Gardner R, Neutzel S (2001) Multi-organ, multi-lineage engraftment by a single bone marrow-derived stem cell. Cell 105:369–377
14. Ianus A, Holz GG, Theise ND, Hussain MA (2003) In vivo derivation of glucose-competent pancreatic endocrine cells from bone marrow without evidence of cell fusion. J Clin Invest 111:843–850
15. Terai S, Sakaida I, Yamamoto N, Omori K, Watanabe T, Ohata S, Katada T (2003) An in vivo model for monitoring transdifferentiation of bone marrow cells into functional hepatocytes. J Biochem Tokyo 134:551–558
16. Okabe M, Ikawa M, Kominami K, Nakanishi T, Nishimune Y (1997) "Green mice" as a source of ubiquitous green cells. FEBS Lett 407:313–319
17. Shinoda K, Mori S, Ohtsuki T, Osawa Y (1992) An aromatase-associated cytoplasmic inclusion, the "stigmoid body," in the rat brain: I. distribution in the forebrain. J Comp Neurol 322:360–376
18. Yamamoto N, Terai S, Ohata S, Watanabe T, Omori K, Shinoda K, Miyamoto K (2004) A subpopulation of bone marrow cells depleted by a novel antibody, anti-Liv8, is useful for cell therapy to repair damaged liver. Biochem Biophys Res Commun 313:1110–1118
19. Watanabe T, Nakagawa K, Ohata S, Kitagawa D, Nishitai G, Seo J, Tanemura S (2002) SEK1/MKK4-Mediated SAPK/JNK signaling participates in embryonic hepatoblast proliferation via a pathway different from NF-kappaB-induced anti-apoptosis Dev Biol 250:332–347
20. Grisham JW, Thorgeirsson SS (1997) Liver stem cells. Academic, Manchester, pp 233–282
21. Petersen BE, Zajac VF, Michalopoulos GK (1998) Hepatic oval cell activation in response to injury following chemically induced periportal or pericentral damage in rates. Hepatology 27:1030–1038
22. Petersen BE, Bowen WC, Patrene KD, Mars WM, Sullivan AK, Murase N, Boggs SS (1999) Bone marrow as a potential source of hepatic oval cells. Science 284:1168–1170
23. Lagasse E, Connors H, Al-Dhalimy M, Reitsma M, Dohse M, Osborne L, Wang X (2000) Purified hematopoietic stem cells can differentiate into hepatocyes in vivo. Nat Med 6:1229–1234
24. Uchida N, Fujisaki T, Eaves AC, Eaves CJ (2001) Transplantable hematopoietic stem cells in human fetal liver have a CD34(+) side population (SP) phenotype. J Clin Invest 108:1071–1077
25. Pittenger MF, Mackay AM, Beck SC, Jaiswal RK, Douglas R, Mosca JD, Moorman MA (1999) Multilineage potential of adult human mesenchymal stem cells. Science 284:143–147
26. Kinoshita T, Miyajima A (2002) Cytokine regulation of liver development. Biochim Biophys Acta 1592;303–312
27. Sakaida I, Terai S, Yamamoto N, Aoyama K, Ishikawa T, Nishina H, Okita K (2004) Transplantation of bone marrow cells reduces CCl_4-induced liver fibrosis in mice. Hepatology 40:1304–1311
28. Wang X, Willenbring H, Akkari Y, Torimaru Y, Foster M, Al-Dhalimy M, Lagasse E (2003) Cell fusion is the principal source of bone-marrow-derived hepatocytes. Nature 422:897–901
29. Vassilopoulos G, Wang PR, Russell DW (2003) Transplanted bone marrow regenerates liver by cell fusion. Nature 422:901–904
30. Tran SD, Pillemer SR, Dutra A, Barrett AJ, Brownstein MJ, Key S, Pak E (2003) Differentiation of human bone marrow-derived cells into buccal epithelial cells in vivo: a molecular analytical study. Lancet 361:1084–1088
31. Schena M, Shalon D, Davis RW, Brown PO (1995) Quantitative monitoring of gene expression patterns with a complementary DNA microarray. Science 270:467–470
32. Xiao L, Wang K, Teng Y, Zhang J (2003) Component plane presentation integrated self-organizing map for microarray data analysis. FEBS Lett 538:117–124
33. Omori K, Terai S, Ishikawa T, Aoyama K, Sakaida I, Nishina H (2004) Molecular signature associated with plasticity of bone marrow cells under prsistent liver damage by self-organizing-map-based gene expression. FEBS Lett 578:10–20

for the small GTPase Rab5, is implicated in endosomal dynamics. *Hum. Mol. Genet.* **12**, 1671–1687.

Saito, K., Murai, J., Kajiho, H., Kontani, K., Kurosu, H., and Katada, T. (2002). A novel binding protein composed of homophilic tetramer exhibits unique properties for the small GTPase Rab5. *J. Biol. Chem.* **277**, 3412–3418.

Schmidt, A., and Hall, A. (2002). Guanine nucleotide exchange factors for Rho GTPases: Turning on the switch. *Genes Dev.* **16**, 1587–1609.

Tall, G. G., Barbieri, M. A., Stahl, P. D., and Horazdovsky, B. F. (2001). Ras-activated endocytosis is mediated by the Rab5 guanine nucleotide exchange activity of RIN1. *Dev. Cell* **1**, 73–82.

Topp, J. D., Gray, N. W., Gerard, R. D., and Horazdovsky, B. F. (2004). Alsin is a Rab5 and Rac1 guanine nucleotide exchange factor. *J. Biol. Chem.* **279**, 24612–24623.

Vojtek, A. B., Hollenberg, S. M., and Cooper, J. A. (1993). Mammalian Ras interacts directly with the serine/threonine kinase Raf. *Cell* **74**, 205–214.

Yang, Y., Hentati, A., Deng, H. X., Dabbagh, O., Sasaki, T., Hirano, M., Hung, W. Y., Ouahchi, K., Yan, J., Azim, A. C., Cole, N., Gascon, G., Yagmour, A., Ben-Hamida, M., Pericak-Vance, M., Hentati, F., and Siddique, T. (2001). The gene encoding alsin, a protein with three guanine-nucleotide exchange factor domains, is mutated in a form of recessive amyotrophic lateral sclerosis. *Nat. Genet.* **29**, 160–165.

[23] Purification and Analysis of RIN Family-Novel Rab5 GEFs

By Kota Saito, Hiroaki Kajiho, Yasuhiro Araki, Hiroshi Kurosu, Kenji Kontani, Hiroshi Nishina, and Toshiaki Katada

Abstract

The small GTPase Rab5 plays important roles in membrane budding and trafficking in the early endocytic pathways, and the activation of this GTPase is mediated by several guanine nucleotide exchange factors (GEFs) at each of the transport steps. The RIN family has been identified as GEFs for Rab5 and shown to possess unique biochemical properties. The RIN family preferentially interacts with an activated form of Rab5, although it enhances guanine nucleotide exchange reaction. Moreover, biochemical analysis indicates that the RIN family functions as a tetramer. In this chapter, we describe the isolation of the recombinant RIN family via expression in *Spodoptera frugiperda* (Sf9) insect cells and in mammalian cells. In addition, functional analysis is also provided to assess the physiological properties of the RIN family.

METHODS IN ENZYMOLOGY, VOL. 403

0076-6879/05 $35.00
DOI: 10.1016/S0076-6879(05)03023-5

Introduction

The small GTPase Rab5, which cycles between GTP-bound active and GDP-bound inactive states, is involved not only in the homotypic fusion process of early endosomes but also in the budding of clathrin-coated vesicles from plasma membrane and its transport to early endosomes (Zerial and McBride, 2001). The involvement of Rab5 in the many processes indicates that the activation of Rab5 is tightly coupled with the progression of each transport step. In the inactive state, Rab5 forms a cytoplasmic complex with a regulatory protein, Rab GDP-dissociation inhibitor (RabGDI), which prevents an association with improper cellular compartments. However, Rab5 replaces GDP with GTP through its interactions with the guanine nucleotide exchange factors (GEFs) at the target membranes. Rabex-5 was first identified as a mammalian Rab5-GEF, and it contained the sequence homologous to the yeast vacuolar protein-sorting 9 (Vps9) protein (Horiuchi *et al.*, 1997). Vps9p acts as a GEF for Vps21p, a yeast homologue of Rab5 GTPase (Hama *et al.*, 1999). At present, several proteins containing the Vps9 domain that act as GEFs for Rab5 have been identified and considered to regulate certain transport steps in accordance with their regulation and localization (Horiuchi *et al.*, 1997; Kajiho *et al.*, 2003; Otomo *et al.*, 2003; Saito *et al.*, 2002; Tall *et al.*, 2001; Topp *et al.*, 2004).

We recently identified members of a novel family of Rab5-GEFs, RIN2 and RIN3, which contain an Src homology 2 (SH2) domain, proline-rich region, and Ras-association domain in addition to a Vps9 domain (Kajiho *et al.*, 2003; Saito *et al.*, 2002). Intriguingly, the RIN family preferentially interacts with the activated form of Rab5, although it enhances guanine nucleotide exchange reaction on Rab5. Moreover, the RIN family is composed of a homophilic tetramer and interacts with amphyphysin II, which regulates the early steps of the endocytic pathway. This chapter describes the isolation of the recombinant RIN family via expression in *Spodoptera frugiperda* (Sf9) insect cells and in mammalian cells. In addition, a functional analysis is also provided to assess the physiological properties of the RIN family.

Methods

Purification of the FLAG-RIN Family from Sf9 Cells

Construction and Selection of RIN-Containing Baculovirus. Bac-To-Bac Baculovirus Expression Systems were purchased from Invitrogen. pFastBac HTa vectors were mutagenized to FLAG-tagged vectors with polymerase chain reaction (PCR) using following primers.

Sense: 5′ AGGATGACGACGATAAGGATTACGATATCCCAA-CGACC 3′
Antisense: 5′ TGTAATCCATGGTGGCGGTTTCGGACCGAGA-TCCG 3′

Extended double-stranded DNAs were phosphorylated followed by ligation and subcloning. The products were verified by sequencing and renamed pFastBac FLAGa vector. Full-length cDNAs encoding human RIN2 and RIN3 were cloned in the *Eco*RI and *Sal*I sites of the pFastBac FLAGa vectors. These vectors were transformed into DH10Bac competent *Escherichia coli* cells so that bacmids were generated by transposition in *E. coli* cells. The transformed cells were plated in Luria Agar plates containing 50 μg/ml kanamycin, 7 μg/ml gentamicin, 10 μg/ml tetracycline, 100 μg/ml Bluo-gal, and 40 μg/ml isopropyl-β-D-thiogalactopyanoside (IPTG). White colonies were picked up, and the successful transpositions were verified by PCR. The bacmid DNAs were precipitated with the standard alkali method.

Expression of the RIN Family in Sf9 Cells. Sf9 cells were grown in EXCELL 420 (JRH Biosciences) medium supplemented with 100 IU/ml penicillin and 100 μg/ml streptomycin at 27° in a 500-ml glass bottle with stirring. Sf9 cells (approximately 10^6 cells) were attached in a 35-mm well plate and transfected with bacmids using CellFECTIN reagents (Invitrogen). After 72 h, virus stocks were harvested by centrifuging at 500×*g* for 5 min. To amplify virus stocks, Sf9 cells attached in plates were infected with virus at a multiplicity of infection of 0.01–0.1 for 48 h. Amplification of virus was done twice to obtain higher-titer virus. To produce FLAG-tagged RIN proteins, Sf9 cells were grown to a density of 5×10^6 cells/ml in a 500-ml glass bottle with stirring. The cells were infected at a multiplicity of infection of 5–10 and incubated for 120 h. The cells were harvested and washed twice with phosphate-buffered saline (PBS) and frozen in liquid N_2 before storage at −80°.

Purification of the RIN Family from Sf9 Cells. For purification of FLAG-tagged RIN proteins from Sf9 cells, the cell pellet was resuspended with 25 ml of an extraction buffer consisting of 40 m*M* *N*-2-hydroxyethylpiperazine-*N*′-2-ethanesulfonic acid (HEPES)-NaOH, pH 7.4, 75 m*M* NaCl, 15 m*M* NaF, 1 m*M* Na_3VO_4, 10 m*M* $Na_4P_2O_7$, 2 m*M* EDTA, 1 μg/ml leupeptin, and 2 μg/ml aprotinin, and subsequently mixed with 25 ml of the extraction buffer containing 2% (w/v) Nonidet P-40 (NP-40). The cell lysate was rotated for 15 min at 4° and then centrifuged at 108,000×*g* for 30 min with an angle rotor. The supernatants were collected and applied to a Bio-Rad open column loaded with Sepharose CL4B (bed volume: 1 ml, Amersham Biosciences). Fractions flowed

through the column were collected and then incubated with a 500-μl bed volume of anti-FLAG M2 agarose beads (Sigma). After being rotated for 90 min at 4°, the mixture was applied to the open column. The flow-through fraction was again loaded to the column to ensure the maximum binding of RIN proteins to the column. The column was washed twice with 5 ml of a wash buffer consisting of 40 m*M* Tris–HCl (pH 8.0), 1 m*M* EDTA, 100 m*M* NaCl, and 0.6% (w/v) 3-[(3-cholamidopropyl) dimethylammonio]-1-propanesulfonic acid (CHAPS). The protein-bound beads were suspended in 1 ml of the wash buffer containing 100 μg/ml FLAG peptide (Sigma) and further incubated for 30 min at 4° with occasional vortexing. The eluted fraction was collected, and the beads were further eluted with 1.5 ml of the elution buffer. To remove the FLAG peptide from eluted fractions, the whole fractions were applied to the PD-10 column (Amersham Biosciences) that had been equilibrated with the wash buffer. The void-volume fractions containing RIN proteins were frozen in liquid N_2 and stored at −80°. A half-liter culture of the infected Sf9 cells yields approximately 200–300 μg of FLAG-tagged RIN proteins (Fig. 1A, top panel).

Assays for Guanine-Nucleotide Exchange and GDP-Dissociation Reactions

Materials. Prenylated Rab5b was purified from baculovirus-infected Sf9 cells according to the method described by Horiuchi *et al.* (1995, see Fig. 1A, bottom), with slight modification: GDP was added to each buffer at a final concentration of 10 μ*M*. Purified Rab5b (180 n*M*) was suspended in a buffer consisting of 25 m*M* Tris–HCl (pH 8.0), 25 m*M* NaCl, 1 m*M* EDTA, 5 m*M* $MgCl_2$, 0.5 m*M* dithiothreitol (DTT), and 0.6% (w/v) CHAPS.

GDP-Dissociation Reaction. The dissociation of [^{3}H]GDP was assayed by measuring the decrease in the radioactivity of [^{3}H]GDP-bound Rab5b trapped on the nitrocellulose filters (ADVANTEC). [^{3}H]GDP-bound Rab5b was first made by incubating purified Rab5b (approximately 1 pmol) for 30 min at 30° in a reaction mixture (9.5 μl) consisting of 20 m*M* Tris–HCl (pH 8.0), 62.5 m*M* NaCl, 10 m*M* EDTA, 5 m*M* $MgCl_2$, 0.5 m*M* DTT, 0.36% (w/v) CHAPS, and 5 μ*M* [^{3}H]GDP (10,000 cpm/pmol). After the incubation, 0.5 μl of 600 m*M* $MgCl_2$ was added to give a final concentration of 20 m*M*, and the mixture was immediately cooled on ice to prevent the dissociation of [^{3}H]GDP from Rab5b. The dissociation of [^{3}H]GDP from Rab5b was measured in a reaction mixture (65 μl) consisting of 40 m*M* Tris–HCl (pH 8.0), 62.5 m*M* NaCl, 5 m*M* EDTA, 15 m*M* $MgCl_2$, 0.5 m*M* DTT, 0.36% (w/v) CHAPS, 120 μ*M* unlabeled GDP, and 40 μ*M* GTP in the presence or absence of FLAG-RIN2 and RIN3 (approximately 20 pmol) by incubating at 30° for indicated times. The reaction was stopped

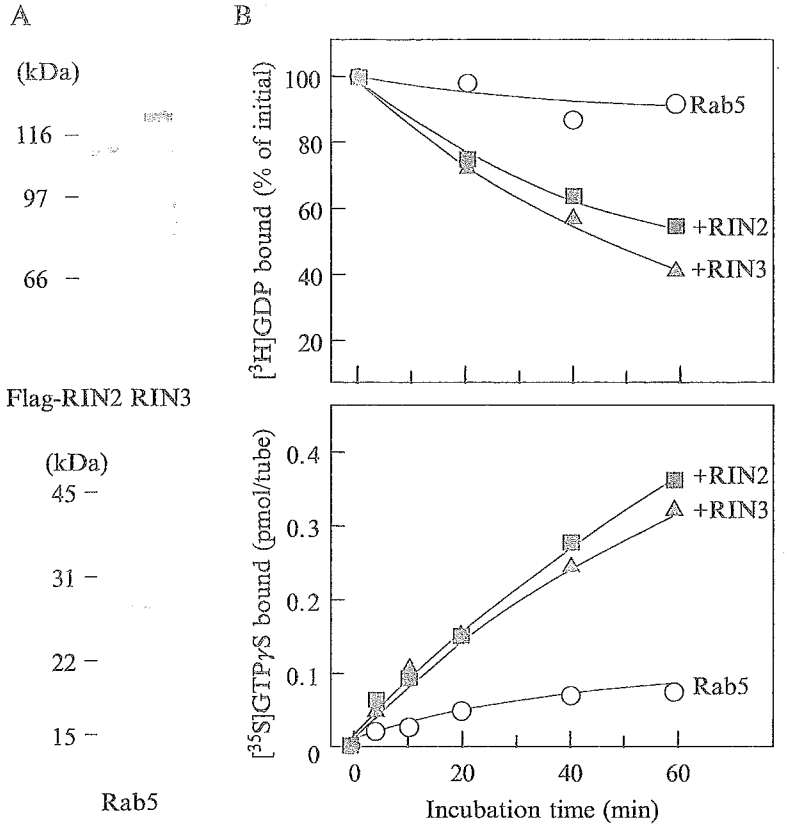

FIG. 1. Analysis of purified RINs and Rab5 by SDS-PAGE and effects of RINs on the guanine-nucleotide exchange reaction of Rab5. (A) Flag-tagged RIN2, RIN3 (top), and prenylated Rab5b (bottom) purified from baculovirus-infected Sf9 cells were separated by SDS-PAGE and stained with Coomassie brilliant blue. (B) Dissociation of [^{3}H]GDP from Rab5b (top) and [^{35}S]GTPγS binding to Rab5b (bottom) were measured in the presence or absence of RINs.

by the addition of approximately 2 ml of an ice-cold buffer consisting of 20 m*M* Tris–HCl (pH 8.0), 20 m*M* $MgCl_2$, and 100 m*M* NaCl, followed by rapid filtration on the nitrocellulose filters. The filters were washed five times with the same ice-cold buffer. After filtration, the radioactivity was counted. As shown in Fig. 1B (top), dissociation of [^{3}H]GDP from Rab5b was markedly stimulated in the presence of RIN2 or RIN3.

Guanine-Nucleotide Binding Reaction. The binding of [^{35}S]GTPγS was assayed by measuring the radioactivity of [^{35}S]GTPγS-bound Rab5b trapped on nitrocellulose filters. To avoid nonspecific guanine-nucleotide binding to various proteins, excess amount (50-fold to GTPγS) of ATP was added to the reaction mixture. Purified Rab5b (approximately

1 pmol) was incubated with RIN2 or RIN3 (15 pmol each) in a reaction mixture (50 μl) consisting of 40 m*M* Tris–HCl (pH 8.0), 62.5 m*M* NaCl, 5 m*M* EDTA, 15 m*M* $MgCl_2$, 0.5 m*M* DTT, 0.36% (w/v) CHAPS, 50 μ*M* ATP, and 1 μ*M* [^{35}S]GTPγS (20,000 cpm/pmol) at 30° for indicated times. The reaction was stopped by the same method as described for the GDP-dissociation reaction. As shown in Fig. 1B (bottom), [^{35}S]GTPγS binding to Rab5b was markedly stimulated in the presence of RIN2 or RIN3.

Assay for In Vitro *Association between the Rab5b and RIN Family*

Preparation of Nucleotide-Bound Forms of Rab5b Proteins. To prepare GTPγS- and GDP-bound forms of Rab5b, the purified protein was incubated with the nucleotides (250 μ*M*) at 30° for 45 min in 11.2 m*M* Tris–HCl (pH 8.0), 50 m*M* HEPES-NaOH (pH 7.5), 110 m*M* NaCl, 0.5 m*M* DTT, 0.27% (w/v) CHAPS, 5 m*M* EDTA, and 2.2 m*M* $MgCl_2$. The reaction was terminated by adding $MgCl_2$ to the final concentration of 10 m*M*.

Expression of the FLAG-RIN Family in Mammalian Cells. COS7 or HeLa cells were maintained in Dulbecco's modified Eagle's medium (DMEM) supplemented with 10% fetal calf serum (FCS), 0.16% (w/v) $NaHCO_3$, 0.6 mg/ml L-glutamine, 100 IU/ml penicillin, and 100 μg/ml streptomycin at 37° in 95% air and 5% CO_2. For cell electroporation with FLAG-RIN2 or RIN3, the cells (1×10^7 cells) were trypsinized and washed twice with 20 ml of Opti-MEM (Invitrogen) and resuspended in 0.2 ml of Opti-MEM. The cell suspension was mixed with 10 μg of plasmids and transferred to a 0.4-cm gap cuvette (Bio-Rad) and incubated on ice for 15 min. The cells were resuspended and electroporated at 220 V, 960 μF with a Bio-Rad Gene Pulser. The cells were diluted with 20 ml of DMEM and cultured for 2 days at 37°.

Purification of the FLAG-RIN Family from COS7 Cells. The transfected COS7 cells were washed twice with PBS and solubilized with Buffer A consisting of 40 m*M* HEPES-NaOH (pH 7.4), 75 m*M* NaCl, 15 m*M* NaF, 1 m*M* Na_3VO_4, 10 m*M* $Na_4P_2O_7$, 2 m*M* EDTA, 1 μg/ml leupeptin, 2 μg/ml aprotinin, and 1% (w/v) NP-40 by vortexing. After gently rotated for 15 min at 4°, lysates were centrifuged at 20,000×*g* for 15 min at 4°. Supernatants were precleared with 20 μl of anti-mouse IgG agarose beads (50% slurry, American Qualex, Inc.) and immunoprecipitated with 10 μl of the agarose beads that had been conjugated with 0.5 μg of the anti-FLAG monoclonal antibody. The beads were washed three times with 1 ml of 20 m*M* Tris–HCl (pH 7.5), 150 m*M* NaCl, and 1% (w/v) NP-40, and three more times with a

buffer consisting of 50 m*M* HEPES-NaOH (pH 7.5), 100 m*M* NaCl, 7.7 m*M* $MgCl_2$, 2 m*M* EDTA, and 0.1% (w/v) NP-40. FLAG-tagged RIN was eluted from the beads with the same buffer containing 1 mg/ml of FLAG peptide.

Assay for In Vitro *Association between the Rab5 and RIN Family.* To assay the association between the Rab5 and RIN family, the GDP- or GTPγS-bound form of Rab5b was mixed with the anti-mouse IgG agarose beads (10 μl) containing FLAG-RIN2, FLAG-RIN3, or FLAG peptide alone and incubated at 25° for 60 min in 0.25 ml of 50 m*M* HEPES-NaOH (pH 7.4), 10 m*M* $MgCl_2$, 5 m*M* EDTA, 0.5 m*M* DTT, 100 m*M* NaCl, and 0.1% (w/v) NP-40. The agarose beads were washed four times with a buffer (500 μl) consisting of 50 m*M* Tris–HCl (pH 8.0), 100 m*M* NaCl, 7 m*M* $MgCl_2$, 2 m*M* EDTA, and 0.2% (w/v) NP-40. Proteins were eluted from the beads with 30 μl of the same buffer containing 1 mg/ml of FLAG peptide. After centrifugation, 24 μl of the supernatant was mixed with 8 μl of 4 × SDS sample buffer, boiled for 5 min, and followed by SDS-PAGE. Immunoblotting was performed with the anti-FLAG M2 monoclonal antibody (Sigma) and the anti-Rab5b polyclonal antibody A-20 (Santa Cruz), respectively.

Gel Filtration Analysis of the RIN Family

Purification of the Recombinant RIN Family from HeLa cells. Transfected HeLa cells were washed twice with PBS and solublized with Buffer A then diluted with Buffer A not containing NP-40 to lower the concentration of NP-40 to 0.5% (w/v). After being gently rotated for 15 min at 4°, lysates were centrifuged at 20,000×*g* for 15 min at 4°. Supernatants were precleared with Sepharose CL4B beads (Amersham Biosciences) and immunoprecipitated with anti-FLAG M2 agarose beads by gently rotating for 2 h at 4°. The beads, being washed three times with 0.5 ml of Tris-buffered saline/0.1% (w/v) NP-40, were further washed three more times with Buffer B consisting of 75 m*M* Tris–HCl (pH 7.5), 1 m*M* EDTA, 100 m*M* NaCl, and 0.2% (w/v) NP-40. For SDS-PAGE analysis, the beads were mixed with 24 μl of Buffer B and 12 μl of 4× sample buffer and boiled for 2 min. The samples were resolved by SDS-PAGE, and immunoblotting was performed with anti-FLAG antibody.

Gel Filtration Analysis of the RIN Family. For gel filtration analysis, the beads were washed six times with 0.5 ml of Buffer C consisting of 25 m*M* Tris–HCl (pH 7.5), 150 m*M* NaCl, and 0.2% (w/v) CHAPS, and subsequently eluted with 0.2 ml of Buffer C containing 1 mg/ml of FLAG peptide by gently vortexing for 1 h at 4°. The eluted fraction was diluted with an

equal volume of Buffer C and applied to a Superdex 200 column (HR 10/30 Amersham Biosciences) that had been equilibrated with Buffer C. Elution was carried out at room temperature at a flow rate of 0.5 ml/min with a fraction volume of 0.25 ml. The fractions were concentrated by precipitation with 10% (final) trichloroacetic acid and subjected to SDS-PAGE and silver staining. The fractions were also analyzed by SDS-PAGE and immunoblotted with anti-FLAG antibody. The elution profile of the column was calibrated with the sizing standards (Oriental Yeast Co. Ltd.) of glutamate dehydrogenase (290 kDa), lactate dehydrogenase (142 kDa), enolase (67 kDa), adenylate kinase (32 kDa), and cytochrome *c* (12.4 kDa).

References

Hama, H., Tall, G. G., and Horazdovsky, B. F. (1999). Vps9p is a guanine nucleotide exchange factor involved in vesicle-mediated vacuolar protein transport. *J. Biol. Chem.* **274**, 15284–15291.

Horiuchi, H., Ullrich, O., Bucci, C., and Zerial, M. (1995). Purification of posttranslationally modified and unmodified Rab5 protein expressed in Spodoptera frugiperda cells. *Methods Enzymol.* **257**, 9–15.

Horiuchi, H., Lippe, R., McBride, H. M., Rubino, M., Woodman, P., Stenmark, H., Rybin, V., Wilm, M., Ashman, K., Mann, M., and Zerial, M. (1997). A novel Rab5 GDP/GTP exchange factor complexed to Rabaptin-5 links nucleotide exchange to effector recruitment and function. *Cell* **90**, 1149–1159.

Kajiho, H., Saito, K., Tsujita, K., Kontani, K., Araki, Y., Kurosu, H., and Katada, T. (2003). RIN3: A novel Rab5 GEF interacting with amphiphysin II involved in the early endocytic pathway. *J. Cell Sci.* **116**, 4159–4168.

Otomo, A., Hadano, S., Okada, T., Mizumura, H., Kunita, R., Nishijima, H., Showguchi-Miyata, J., Yanagisawa, Y., Kohiki, E., Suga, E., Yasuda, M., Osuga, H., Nishimoto, T., Narumiya, S., and Ikeda, J. E. (2003). ALS2, a novel guanine nucleotide exchange factor for the small GTPase Rab5, is implicated in endosomal dynamics. *Hum. Mol. Genet.* **12**, 1671–1687.

Saito, K., Murai, J., Kajiho, H., Kontani, K., Kurosu, H., and Katada, T. (2002). A novel binding protein composed of homophilic tetramer exhibits unique properties for the small GTPase Rab5. *J. Biol. Chem.* **277**, 3412–3418.

Tall, G. G., Barbieri, M. A., Stahl, P. D., and Horazdovsky, B. F. (2001). Ras-activated endocytosis is mediated by the Rab5 guanine nucleotide exchange activity of RIN1. *Dev. Cell* **1**, 73–82.

Topp, J. D., Gray, N. W., Gerard, R. D., and Horazdovsky, B. F. (2004). Alsin is a Rab5 and Rac1 guanine nucleotide exchange factor. *J. Biol. Chem.* **279**, 24612–24623.

Zerial, M., and McBride, H. (2001). Rab proteins as membrane organizers. *Nat. Rev. Mol. Cell Biol.* **2**, 107–117.

Human Molecular Genetics, 2005, Vol. 14, No. 6 1–11
doi:10.1093/hmg/ddi069
Advance Access published on xxx

The *Pax6* isoform bearing an alternative spliced exon promotes the development of the neural retinal structure

Noriyuki Azuma[1,2,*], Keiko Tadokoro[2], Astuko Asaka[2], Masao Yamada[2], Yuki Yamaguchi[3], Hiroshi Handa[3], Satsuki Matsushima[4], Takashi Watanabe[4], Shinichi Kohsaka[5], Yasuyuki Kida[6], Tomoki Shiraishi[6], Toshihiko Ogura[6], Kenji Shimamura[7] and Masato Nakafuku[7]

[1]Department of Ophthalmology, National Center for Child Health and Development, Tokyo 157-8535, Japan, [2]Department of Genetics, National Research Institute for Child Health and Development, Tokyo 154-8567, Japan, [3]Department of Biological Information, Tokyo Institute of Technology, Graduate School of Bioscience and Biotechnology, Yokohama, 226-8501, Japan, [4]Department of Clinical Pathology, Kyorin University School of Medicine, Tokyo 181-8611, Japan, [5]Department of Neurochemistry, National Institute of Neuroscience, Tokyo, 187-8502, Japan, [6]Department of Developmental Neurobiology, Institute of Development, Aging and Cancer, Sendai 980-8575, Japan and [7]Department of Neuroscience, University of Tokyo Graduate School of Medicine, Tokyo 113-0033, Japan

Received November 28, 2004; Accepted January 18, 2005

The vertebrate retina has an area where visual cells are closely packed for proper vision that is known as a fovea, an area centralis or a visual streak. The molecular mechanism that regulates the formation of these structures and visual cell gradients is unknown. The transcription factor Pax6 is a master regulator of eye development. A Pax6 isoform that contains an exon 5a-encoded 14 amino acid insertion in its paired domain, Pax6(+5a), has different DNA-binding properties compared with the Pax6(−5a) isoform. Little is known about the functional significance of Pax6(+5a). Here, we show that Pax6(+5a) is expressed especially in the retinal portion where visual cells accumulate during eye development and, when overexpressed, induces a remarkable well-differentiated retina-like structure. Pax6(+5a) proteins that bear point mutations that are found in patients with foveal hypoplasia are unable to induce these ectopic retina-like structures. We propose that Pax6(+5a) induces a developmental cascade in the prospective fovea, area centralis or visual streak region that leads to the formation of a retinal architecture bearing densely packed visual cells.

INTRODUCTION

Most vertebrates have a region of the retina where cone photoreceptors, bipolar cells and ganglion cells accumulate and specialize, which contributes to better vision (1–3). This region comes in two general forms, namely, a visual streak and an area centralis. Animals that are nocturnal or have relatively poor vision bear a visual streak, where the photoreceptors, bipolar cells and ganglion cells congregate and become specialized along a horizontal line of the eye fundus. In contrast, animals that have relatively good vision bear the area centralis, which is a circular spot in the retina. The image of an object becomes centered on this region. A specialized form of the area centralis is the fovea, which helps many reptiles and birds, and most primates achieve greater visual sensitivity. The fovea is an area in which cone photoreceptors are highly concentrated and the inner retina is thinned. Human patients lacking the fovea have a poor visual acuity of 0.1–0.3, even with lens correction (4,5). Thus, the fovea is an essential architectural feature that is required for our sharp visual acuity.

In most vertebrates that have a fovea or an area centralis, the retinal cells first accumulate, differentiate and form synaptic connections at the prospective fovea or area centralis

*To whom correspondence should be addressed at: Department of Ophthalmology, National Center for Child Health and Development, 2-10-1 Okura, Setagaya-ku, Tokyo 157-8535, Japan. Tel: +81 334160181; Fax: +81 334162222; Email: azuma-n@ncchd.go.jp

region during the very early stages of eye development, corresponding to the time when ganglion cells appear in the retina. The differentiation of the retinal cells then progresses from the centre to the periphery, which results in a gradient of visual sensitivity (2,3). The molecular mechanisms that regulate the formation of these specific retinal structures are not well elucidated, although previous studies have explored mechanism and genes involved in differentiation of the retinal area (6–8).

Recently, patients with foveal hypoplasia were found to bear mutations in the *PAX6* gene (4,5). The *Pax6* gene encodes a transcription factor and plays important roles in eye morphogenesis in both vertebrates and invertebrates (9–12). This gene has been reported to induce ectopic eye formation in *Drosophila melanogaster* (13) and *Xenopus* larvae (14), and is known as a master control gene in eye formation (9–11). Pax6 is expressed in various eye tissues. In the neural retina, Pax6 is expressed widely in multipotent progenitor cells at early stages and to a lesser extent in ganglion, horizontal and amacrine cells at late stages (15–17). The *Pax6* gene produces two isoforms by alternative splicing, namely, Pax6(−5a) and Pax6(+5a). Pax6(+5a) differs from Pax6(−5a) by the presence of an exon 5a-encoded 14 amino acid insertion in its paired-type DNA-binding domain (paired domain, or PD) (18,19). Pax6(−5a) and Pax6(+5a) show distinct DNA-binding properties (20) and their distinct consensus binding sequences have been determined. These are termed P6CON and 5aCON, respectively (21). Mutational analyses have shown that the N-terminal subdomain (NTS) and the C-terminal subdomain (CTS) of the Pax6 PD are respectively responsible for the DNA-binding abilities of Pax6(−5a) and Pax6(+5a) and their transactivation activity (20,22). Pax6(−5a) binds to a promoter element of the ζ-*crystallin* gene at a site that is highly similar to P6CON (23), while target genes of Pax6(+5a) that bear 5aCON-like sequences are yet to be identified.

Many mutations in the *PAX6* gene have been identified in human patients with foveal hypoplasia (4,5,24–27). In most classical aniridia patients, caused by haploinsufficiency of PAX6 due to its deletion or the presence of a nonsense mutation, all other eye tissues apart from the iris, including the cornea, lens, fovea and optic nerve, are also affected. In contrast, missense mutations in the *PAX6* gene cause more specific eye anomalies (4,5,25–27), probably because Pax6 has multiple functional domains and that missense mutations in this gene disturb one or only a few of these domains. Previously, we reported two PAX6 missense mutations, R128C in the CTS of the PD and V54D in exon 5a, in Japanese patients with foveal hypoplasia (4,5). An R128C mutation was again identified in an independent European patient with the same phenotype (26). These findings suggest that the CTS and exon 5a, which are two elements that are thought to be important for the function of the Pax6(+5a) isoform, may be involved in the formation of the fovea. We investigated expression pattern of Pax6(+5a) in the developing retina and effect of the isoform in retinal development by gain-of-function experiments, and here present evidence that Pax6(+5a) contributes to promote the formation of the retinal structure.

RESULTS

Pax6(+5a) is abundantly expressed in the retinal portion where visual cells accumulate

We first examined the regional expression of the Pax6 isoforms by subjecting sections of a neonatal marmoset eye (which has a fovea) to immunohistochemical staining with two different antibodies that can distinguish between the two Pax6 isoforms. One of these antibodies, which is denoted as anti-Pax6, was raised against amino acids 1–223 including those encoded by exon 5a. This antibody reacts with both Pax6(−5a) and Pax6 (+5a), as reported previously (16,17). For this study, we raised another antibody against a synthetic peptide consisting of the 14 amino acid residues that are encoded by exon 5a (anti-exon 5a). Western blotting of proteins prepared from cultured mouse embryonic carcinoma P19 cells that had been transfected with constructs expressing Pax6(−5a) or Pax6(+5a), and of marmoset tissues expressing both isoforms demonstrated the specificity of these antibodies (Fig. 1A). On the marmoset sections, anti-Pax6 visualized three layers, namely, the ganglion cell layer and the inner and outer edges of the inner nuclear layer of the retina. The foveal region was heavily stained, and both the nasal and temporal nasal sides were also stained (Fig. 1C, middle panels). This indicates the wide distribution of Pax6 proteins throughout the entire retina. In contrast, the anti-exon 5a staining pattern suggested that the Pax6(+5a) protein localizes to a restricted retinal area between the optic nerve head and the fovea (Fig. 1C b and c). This was clear when the staining in the nasal and foveal sides of the optic nerve head was compared. The staining was identified scarcely in the nasal side but obviously in the foveal side (Fig. 1C b). From these observations, we conclude that the Pax6(+5a) isoform is expressed especially in the restricted retinal portion where the densely packed visual cells reside.

Reflecting evolutionary conservation of the amino acid sequence encoded by exon 5a, the anti-exon 5a antibody reacts with chicken Pax6(+5a) as well, albeit weakly. In the chicken retina of Hamburger–Hamilton (HH) stage 45, the Pax6(+5a) protein appears to localize in a restricted retinal area of the visual streak, whereas the Pax6(−5a) protein distributes throughout the entire retina (Fig. 2A). To compare the expression levels of the two isoforms, we next performed semi-quantitative RT–PCR analysis using dissected retinal tissues of chick embryos at HH stages 12–45. The isolated RNAs were subjected to RT–PCR analysis using specific primers that flank exon 5a and can distinguish between the two isoforms *Pax6(+5a)* and *Pax6(−5a)*. At an early developmental stage (HH stage12), when the optic vesicle is formed and multipotent progenitor cells still exist in the neural retina, the two isoforms were expressed in both the central nervous system (CNS) and the eye primordium but the *Pax6(−5a)* isoform predominated (Fig. 2B). At HH stage 20, Pax6(−5a) was still the major transcript. At this stage, the formation of the eye is proceeding and lens formation is evident. During HH stages 24–30, the ganglion cells in the retina differentiate. The level of *Pax6(−5a)* expression seems to decrease transiently at HH stage 24 and increase at HH stage 30. Interestingly, the level of *Pax6(+5a)* expression gradually increased during this period

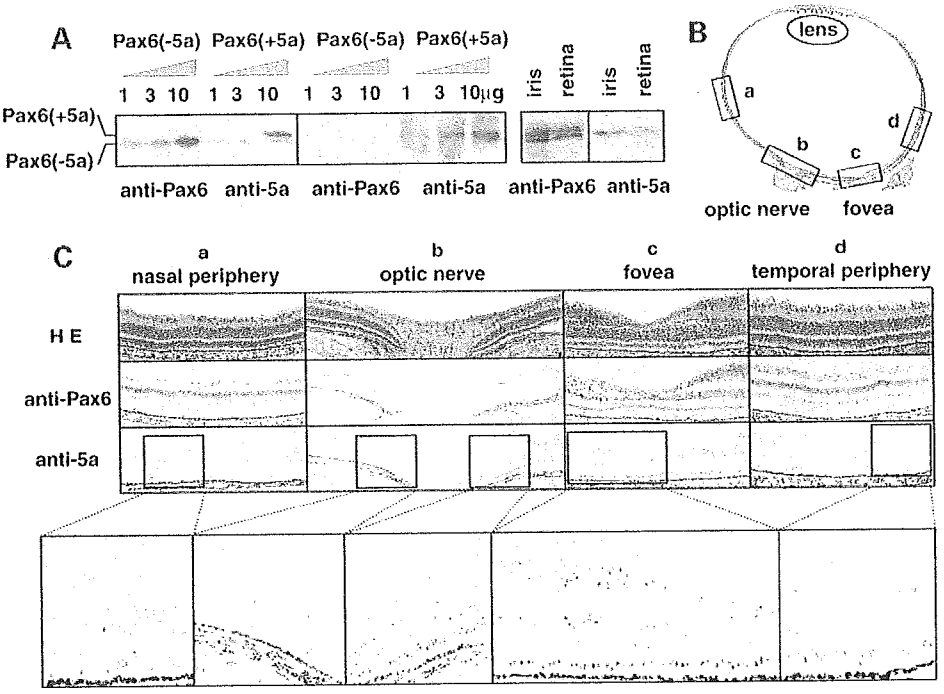

Figure 1. Histochemical analysis of the expression of the two Pax6 isoforms in the neonatal marmoset eye. (**A**) Western blotting analysis confirming the specificity of the two antibodies that were used. P19 cells (10^5 cells) were transfected with either the Pax6(−5a) or Pax6(+5a) expression construct and nuclear protein fractions obtained 24 h post-transfection were analyzed. Anti-Pax6 recognized the exogenously expressed Pax6(−5a) and Pax6(+5a) proteins as well as endogenous Pax6(−5a) protein, whereas anti-exon 5a recognized Pax6(+5a) but not Pax6(−5a). Western blotting analysis of nuclear fraction proteins obtained from the iris and retina tissues of the neonatal marmoset (*Callithrix jacchus*) also showed that anti-Pax6 recognized both native Pax6(−5a) and Pax6(+5a) proteins, whereas anti-exon 5a recognized Pax6(+5a) but not Pax6(−5a). (**B**) View of a horizontal section of the eye of a neonatal marmoset stained with HE. (**C**) Magnified fields of the eye stained with HE, anti-Pax6 or anti-exon 5a (bar scale 100 μm). Further enlarged images are shown below. a, nasal peripheral area; b, optic nerve head area; c, fovea area; d, temporal peripheral area. The staining for anti-exon 5a localizes around the fovea area, whereas that for anti-Pax6 is detected throughout the entire retina. The result shown is representative of three independent experiments using four marmoset eyes.

in all ocular tissues such as the cornea, lens and retina. Increased expression of *Pax6(+5a)* was also evident in the retina in later stages (HH stages 36–45), when all photoreceptors, horizontal and amacrine cells differentiate. Although the eyes of domestic birds lack the fovea, they possess a distinct visual streak in the posterior portion of the retina (1,2). Expression of *Pax6(+5a)* became particularly intense in this posterior portion. At HH stage 36, the expression of *Pax6(+5a)* exceeded that of *Pax6(−5a)* in the posterior retina. These observations indicate that expression of the two Pax6 isoforms are differentially regulated during retinal development, with Pax6(+5a) expression increasing only in a specified region, whereas Pax6(−5a) expression being throughout the retina.

In *ovo* misexpression of *Pax6(+5a)* gene markedly expands the retinal layer and promotes the growth and differentiation of retinal cells into visual cells

Next, we investigated the roles the two Pax6 isoforms play in the formation of the eye architecture by *in ovo* electroporation (28). Thus, an expression construct for either Pax6(+5a) or Pax6(−5a) was electroporated into the developing retina of HH stages 16–30 chick embryos, together with an expression construct of green fluorescence protein (GFP) (29) to monitor the expression of the transgenes. Expression plasmids [pCAGGS-PAX6(−5a) and pCAGGS-PAX6(+5a)] carry the entire human *PAX6* coding region with or without exon 5a under the control of a cytomegalovirus enhancer and chicken β-actin promoter, as described previously (5,22). Embryos that had been electroporated were harvested at various stages and analyzed. Retinal formation was scarcely affected when either isoform was transduced after HH stage 30 (data not shown). However, marked changes were observed when either isoform was transduced at HH stages 16–24, when the formation of the optic cup was completed. Six to twelve hours after electroporation of Pax6(−5a) and GFP (HH stage 18), the electroporated region, confirmed by staining with anti-Pax6 and anti-GFP antibodies, was found to proliferate excessively, as evidenced by intense staining with anti-5-bromo-2′-deoxyuridine (BrdU) antibody (Fig. 3). The promotion of retinal cell proliferation occurred similarly up to this stage regardless of the Pax6 isoforms overexpressed (data not shown). Electroporation of the empty vector alone, the pCAGGS-GFP or both constructs did not induce any change.

At later stages, a significant difference in the effect of the two Pax6 isoforms was observed. When Pax6(−5a) was misexpressed, 3–7 days after the electroporation (HH stages 28–35), 47% ($n = 198$) of the eyes were larger than the untreated